

Adsorption and Photocatalytic Degradation of Toluene Vapor in Air on Highly Hydrophobic TiO₂ Pillared Clay

Chihiro Ooka,* Hisao Yoshida,[†] Kenzi Suzuki,^{††} and Tadashi Hattori[†]

Nagoya Municipal Industrial Research Institute, 3-4-41, Rokuban, Atsuta-ku, Nagoya 456-0058

[†]Department of Applied Chemistry, Graduate School of Engineering, Nagoya University, Furo-cho, Chikusa-ku, Nagoya 464-8603

^{††}Ceramics Research Institute, National Institute of Advanced Industrial Science and Technology, 2266-98, Anagahora, Shimoshidami, Moriyama-ku, Nagoya 463-8560

(Received May 22, 2003; CL-030454)

Hydrophobicity of TiO₂ pillared clay prepared from different raw clays increased with the order of the raw clay; saponite < montmorillonite < fluorine mica. This order agreed with that of performance in both adsorption and photocatalytic degradation of toluene vapor in humid air.

TiO₂ pillared clay has attracted much attention as a new type of photocatalyst since its superior adsorption property accelerates photocatalytic reaction.¹⁻⁵ We have investigated the photocatalytic degradation of organic substance on TiO₂ pillared clay in water.^{1,2} In the previous paper, it was clarified that interlayer surface of TiO₂ pillared clay is hydrophobic and hydrophobic interaction largely affects adsorption and photocatalytic degradation of phthalate esters and bisphenol-A in water on TiO₂ pillared clay.¹ Murayama et al. also reported that hydrophobicity of TiO₂ pillared clay affected photocatalytic degradation of hexachlorocyclohexane in water.³ In the present work, to know the influence of hydrophobicity of the TiO₂ pillared clay on the photocatalytic activity in degradation of toluene vapor in air, we prepared three kinds of TiO₂ pillared clay using different raw clays.

TiO₂ pillared clays were prepared with a procedure reported by Kitayama et al.⁴ with some modifications. Titanium tetraisopropoxide was added to stirred acetic acid solution of 80 wt %. The molar ratio of acetic acid to the alkoxide was 24. The resulting white slurry was stirred at room temperature to give clear TiO₂ sol. The raw clays used were synthetic saponite (Smecton SA, Kunimine Industrial Company), natural refined montmorillonite (Kunipia-F, Kunimine Industrial Company) and synthetic fluorine mica (Somasif ME-100, COOP Chemical Co, Ltd.), and those cation exchange capacity (CEC) were 1.1, 1.2, and 0.7 meq·g⁻¹, respectively. The TiO₂ sol was mixed with 1 wt % aqueous suspension of the raw clay. The mixed suspension was stirred for 3 h at room temperature. The product was centrifuged and washed with water several times for re-

moving excess TiO₂ sol. The aqueous suspension of the washed wet product was sprayed on one side of a circular filter paper (Advantec Toyo, No. 5A, 110 mm diameter) to prepare the test piece for adsorption-photocatalytic degradation test. The test piece was dried in air at room temperature and followed by heating at 393 K. The catalysts prepared are listed in Table 1. Each TiO₂ pillared clay will be referred to as Sapo-Ti, Mont-Ti and Mica-Ti in this letter. P-25 (Degussa) was employed as a reference TiO₂ catalyst.

From results of X-ray diffraction (XRD), every pillared clay showed similar interlayer spacing, which ranged from 48 to 56 Å (Table 1). Further, every pillared clay showed clear and similar intensity of diffractions due to anatase phase in addition to those due to the host clay. Crystalline size of TiO₂ of the pillared clay, which calculated from anatase (101) diffraction, varied from 36 to 39 Å and its range was narrow (Table 1). These results indicated that TiO₂ nanoparticles were intercalated to silicate layers in the clay to expand layer spacing, and that the crystalline state and size of anatase were similar in every pillared clay.

Nitrogen adsorption isotherm was measured at 77 K using the pillared clay degassed at 393 K. In Table 1, BET surface area calculated from nitrogen adsorption isotherm varied from 301 to 402 m²g⁻¹ and total pore volume ranged from 0.264 to 0.329 cm³g⁻¹. TiO₂ content varied from 41.7 to 48.0 wt % (Table 1). These variations of BET surface area, total pore volume and TiO₂ content should be due to difference in particle size or CEC of the raw clays. Meanwhile average pore diameter and interlayer spacing varied only slightly as shown in Table 1. Therefore, the structures of interlayer pores in the pillared clays, which would affect adsorption property of the catalysts, seem to make little difference.

Water adsorption isotherm was measured at 298 K using the pillared clay degassed at 393 K. The extent of hydrophobicity on the catalyst was evaluated by using surface hydrophobicity index (SHI),⁶ which was calculated from both BET surface area

Table 1. Results of characterization of the TiO₂ pillared clays prepared and reference material

Catalyst	Interlayer Spacing ^a / Å	Crystalline size of TiO ₂ ^b / Å	Average pore diameter ^c / Å	Total pore volume ^c / cm ³ g ⁻¹	BET surface area in N ₂ adsorption ^c / m ² g ⁻¹	BET surface area in H ₂ O adsorption ^d / m ² g ⁻¹	SHI ^e / %	TiO ₂ content ^f / wt %
Sapo-Ti	56	39	31	0.283	368	324	12	48.0
Mont-Ti	48	36	35	0.264	301	239	21	43.5
Mica-Ti	55	39	42	0.329	402	268	33	41.7
P-25 ^g	—	197	—	0.097	49	39	20	99.4

^aObtained by subtracting the thickness of silicate layer (9.6 Å) from *d*-spacing of (001) of silicate layers. ^bCalculated from (101) diffraction of anatase using the Scherrer's equation. ^cDetermined from nitrogen adsorption isotherm at 77 K. ^dDetermined from water adsorption isotherm at 298 K. ^eSurface hydrophobicity index was obtained by the following equation: SHI (%) = (1 - BET surface area in H₂O adsorption / BET surface area in N₂ adsorption) × 100. ^fDetermined by elemental analysis using X-ray fluorescence method. ^gDegussa.

obtained by nitrogen and water adsorption isotherms (Table 1). SHI on the pillared clay ranged from 12 to 33% and was raised in order of Sapo-Ti < Mont-Ti < Mica-Ti.

Weight of the catalyst on the test piece for adsorption-photocatalytic degradation test was in the range from 21 to 33 mg. The test piece was irradiated by UV light for 24 h in air for cleaning up the catalyst surface before the test. The test piece was put in a gas sampling bag made of polyvinyl fluoride (Tedlar) film having 5 L capacity and the bag was sealed. 3 L of toluene gas regulated to 120 ppm with air, which contained 20–30% relative humidity, was introduced into the bag through a valve and stopped. The bag was set in the dark at room temperature. A part of the gas was extracted with a syringe through a valve for monitoring the toluene concentration. The monitoring was achieved by means of gas chromatography (GC-FID), and then adsorption equilibrium concentration was checked. The adsorption to the support filter paper was confirmed by the blank test and subtracted. After the adsorption equilibrium was achieved in the dark, UV irradiation (black light, wave length of the maximum intensity: 365 nm, illumination at the surface of the bag: $1.0 \text{ mW} \cdot \text{cm}^{-2}$) was carried out at room temperature. The toluene concentration was monitored in the same manner as above and CO_2 concentration was also monitored by means of GC-TCD.

Figure 1a shows adsorption amount of toluene on the catalysts. The three kinds of pillared clays showed different adsorption performance: the order of adsorption amount was Mica-Ti > Mont-Ti > Sapo-Ti. This order was the same as the order of SHI (Table 1). This indicated that high surface hydrophobicity enhanced enrichment of hydrophobic toluene vapor by adsorption on the surface with less inhibition by adsorption of water vapor in air. Figure 1b shows degradation rate constants in the initial stage on the catalysts. The order of the rate constant among the pillared clays was quite the same order of the adsorption amount. Especially, Mica-Ti, which had the highest surface hydrophobicity among the catalysts, showed the most excellent photocatalytic performance, namely, about five times of P-25. Figure 2 shows amount of produced CO_2 in degradation per weight of the catalyst. The order of amount of produced CO_2 was also agreed with that of the degradation rate constant. After 180 min of irradiation, mineralized toluene reached 86% of initial amount in degradation on Mica-Ti. As mentioned above (results of XRD), the crystalline phase and the size of TiO_2 in every pillared clay seemed to be similar to each other. Therefore,

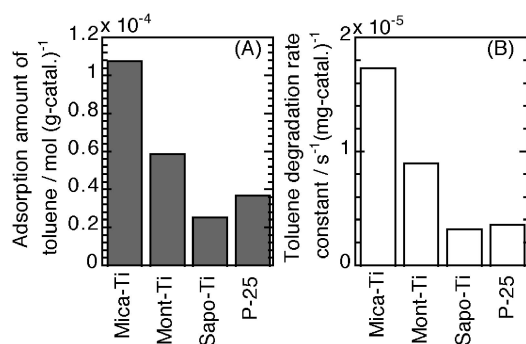


Figure 1. Adsorption amount (A) and initial reaction rate constant (B) per weight of catalyst in adsorption-photocatalytic degradation test of toluene vapor on Mica-Ti, Mont-Ti, Sapo-Ti, and P-25.

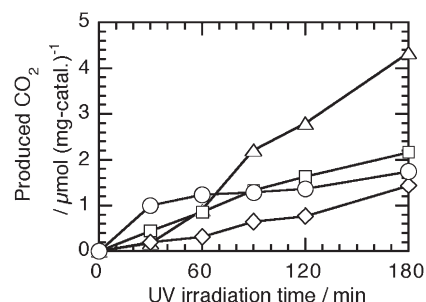


Figure 2. Time course of amount of produced CO_2 in photocatalytic degradation test of toluene vapor on Mica-Ti (triangle), Mont-Ti (square), Sapo-Ti (diamond), and P-25 (circle).

this difference in photocatalytic activity on the pillared clay seems to be due to the difference in surface hydrophobicity of the pillared clay. Further, it was confirmed that enrichment of hydrophobic reactant by adsorption enhances photocatalytic degradation in humid air. In literature, negative effects of humidity were reported on degradation rate of hydrophobic substance in air.⁷ To protect photocatalytic performance of TiO_2 from the inhibition by water vapor adsorption, the enhancement of surface hydrophobicity of the catalyst by selection of host clay around TiO_2 seems to be one of the effective means.

In conclusion, it was clarified in the present study that the hydrophobicity of pillared clay could be designed by the selection of raw clay and highly hydrophobic TiO_2 pillared clay has an advantage for the photocatalytic performance in degradation of toluene in air through enrichment of the substance by adsorption.

This work was partially supported by a subsidy of the Small and Medium Enterprise Agency, Japan, by a Grant-in-Aid for scientific research on priority areas (A) "The environmental risk of endocrine disruptor", from the Ministry of Education, Culture, Sports, Science and Technology, Japan, and by the Hibi Research Grant.

References

- 1 C. Ooka, H. Yoshida, M. Horio, K. Suzuki, and T. Hattori, *Appl. Catal., B*, **41**, 313 (2003).
- 2 C. Ooka, S. Akita, Y. Ohashi, T. Horiuchi, K. Suzuki, S. Komai, H. Yoshida, and T. Hattori, *J. Mater. Chem.*, **9**, 2943 (1999); H. Yoshida, T. Kawase, Y. Miyashita, C. Murata, C. Ooka, and T. Hattori, *Chem. Lett.*, **1999**, 715.
- 3 H. Murayama, K. Shimizu, N. Tsukada, A. Shimada, T. Kodama, and Y. Kitayama, *Chem. Commun.*, **2002**, 2678.
- 4 Y. Kitayama, T. Kodama, M. Abe, H. Shimotsuma, and Y. Matsuda, *J. Porous Mater.*, **5**, 121 (1998); T. Kaneko, M. Fujii, T. Kodama, and Y. Kitayama, *J. Porous Mater.*, **8**, 99 (2001); K. Shimizu, T. Kaneko, T. Fujishima, T. Kodama, H. Yoshida, and Y. Kitayama, *Appl. Catal., A*, **225**, 185 (2002).
- 5 J. Sterte, *Clays Clay Miner.*, **34**, 658 (1986); S. Yamanaka, T. Nishihara, M. Hattori, and Y. Suzuki, *Mater. Chem. Phys.*, **17**, 87 (1987); H. Yoneyama, S. Haga, and S. Yamanaka, *J. Phys. Chem.*, **93**, 4833 (1989); A. Bernier, L. F. Admaia, and P. Grange, *Appl. Catal.*, **77**, 269 (1991); L. Khalfallah Boudali, A. Ghorbel, D. Tichit, B. Chiche, R. Dutartre, and F. Figueras, *Microporous Mater.*, **2**, 525 (1994); Z. Ding, H. Y. Zhu, G. Q. Lu, and P. F. Greenfield, *J. Colloid Interface Sci.*, **209**, 193 (1999); M. A. Vicente, M. A. Banares-Munoz, R. Torenz, L. M. Gandia, and A. Gil, *Clay Miner.*, **36**, 125 (2001).
- 6 F. H. Healey, Y.-H. Yu, and J. J. Chessick, *J. Phys. Chem.*, **59**, 399 (1955); A. C. Zettlemoyer, *Off. Dig., Fed. Soc. Paint Technol.*, **29**, 1238 (1957).
- 7 L. A. Phillips and G. B. Raupp, *J. Mol. Catal.*, **77**, 297 (1992); S. Kutsuna, Y. Ebihara, K. Nakamura, and T. Ibusuki, *Atmos. Environ.*, **27A**, 599 (1993).